Electronic Supplementary Information

Influence of nitrosyl coordination on the binding mode of quinaldate in selective ruthenium frameworks. Electronic structure and reactivity aspects

Abhishek Dutta Chowdhury, Prinaka De, Shaikh M. Mobin, and Goutam Kumar Lahiri*

Department of Chemistry, IIT Bombay, Powai, Mumbai-400076, India, Fax: 91-022-2572-3480, E-mail: lahiri@chem.iitb.ac.in

Table S1 Comparison of DFT calculated selected bond distances and bond angles of $\{RuNO\}^n$ (n = 6,7)

Bond distance (Å)/Bond angle (°)	$[\mathbf{1}]^+$	**1**	$[\mathbf{2}]^{2+}$	$[\mathbf{2}]^+$
Ru-N(1)	–	–	2.19	2.21
Ru-N(2)	2.11	2.10	2.14	2.13
Ru-N(3)	2.03	2.02	2.02	1.99
Ru-N(4)	2.11	2.11	2.13	2.13
Ru-N(5)	1.79	1.93	1.80	1.92
Ru-O(1)	2.05	2.10	1.97	2.06
Ru-Cl	2.44	2.46	–	–
C(1)-O(1)	1.30	1.29	1.34	1.31
C(1)-O(2)	1.24	1.24	1.21	1.22
N(5)-O(3)	1.14	1.18	1.15	1.18
N(1)-Ru-N(3)	–	–	160.82	166.11
N(2)-Ru-N(4)	156.32	157.16	158.22	158.00
O(1)-Ru-N(5)	97.80	94.48	175.03	177.37
N(3)-Ru-N(5)	175.95	177.82	94.98	90.44
Cl-Ru-O(1)	171.59	175.01	–	–
N(5)-Ru-N(2)	100.80	100.74	90.86	91.96
N(5)-Ru-N(3)	175.95	177.82	94.98	90.44
N(5)-Ru-N(4)	102.88	102.09	95.83	92.37
N(5)-Ru-N(1)	–	–	104.18	103.45
N(1)-Ru-N(4)	–	–	99.17	92.37
N(3)-Ru(1)-O(1)	86.11	87.63	81.61	86.94
Ru-N(5)-O(3)	170.25	141.85	174.02	139.69

Table S2(a) Selected molecular orbital composition for [**1**]$^{+}$ in S=0 state

MOs	Energy	Composition (%)				
		Ru	NO	trpy	L	Cl
LUMO+6	−4.39	7	0	91	1	1
LUMO+5	−4.45	8	0	92	0	1
LUMO+4	−4.48	42	3	49	4	2
LUMO+3	−5.35	20	34	44	2	0
LUMO+2	−5.47	2	0	98	0	0
LUMO+1	−5.88	23	63	13	1	0
LUMO	−6.07	11	42	39	5	3
HOMO	−8.35	1	0	0	99	0
HOMO-1	−8.88	7	0	0	87	6
HOMO-2	−9.04	8	0	1	84	7
HOMO-3	−9.09	28	1	2	27	42
HOMO-4	−9.40	12	5	2	5	76
HOMO-5	−9.92	4	0	2	90	4
HOMO-6	−10.04	18	1	18	33	30

Table S2(b) Selected molecular orbital composition for [**2**]$^{2+}$ in S=0 state

MOs	Energy	Composition (%)			
		Ru	NO	trpy	L
LUMO+6	−7.42	46	12	22	20
LUMO+5	−7.87	31	1	28	40
LUMO+4	−7.92	32	1	28	39
LUMO+3	−8.33	2	1	97	0
LUMO+2	−8.64	8	6	84	2
LUMO+1	−9.41	26	65	5	4
LUMO	−9.43	24	62	8	6
HOMO	−12.16	4	0	1	95
HOMO-1	−12.70	0	0	1	99
HOMO-2	−12.80	3	2	0	95
HOMO-3	−13.07	1	1	97	1
HOMO-4	−13.29	17	10	12	61
HOMO-5	−13.81	58	2	15	25
HOMO-6	−13.83	12	7	75	6

Table S3(a) Selected molecular orbital composition for **1** in S=1/2 state

MOs	Energy	Composition of α-MO.s (%)				
		Ru	NO	trpy	L	Cl
LUMO+2	−1.30	2	1	45	52	0
LUMO+1	−2.24	3	0	97	0	0
LUMO	−2.29	12	5	82	0	1
SOMO	−4.02	26	43	17	10	4
HOMO-1	−5.091	52	1	5	10	32
HOMO-2	−5.663	18	12	4	16	50
MOs	Energy	Composition of β-MO.s (%)				
		Ru	NO	trpy	L	Cl
LUMO+2	−1.30	3	2	13	82	0
LUMO+1	−2.22	2	0	98	0	0
LUMO	−2.36	3	44	50	2	1
HOMO	−5.05	53	0	5	11	31
HOMO-1	−5.43	38	7	0	5	50
HOMO-2	−5.85	5	4	1	90	0

Table S3(b) Selected molecular orbital composition for [**2**]$^{+}$ in S=1/2 state

MO	Energy	Composition of α-MO.s (%)			
		Ru	NO	trpy	QA
LUMO+2	−4.72	3	0	2	95
LUMO+1	−5.18	1	1	97	1
LUMO	−5.42	3	5	90	2
SOMO	−7.16	32	51	5	12
HOMO-1	−8.97	43	4	9	44
HOMO-2	−9.05	22	10	3	65
MO	Energy	Composition of β-MO.s (%)			
		Ru	NO	trpy	QA
LUMO+2	−4.74	3	3	2	92
LUMO+1	−5.18	1	1	98	0
LUMO	−5.42	3	91	4	2
HOMO	−8.70	47	13	6	34
HOMO-1	−8.96	48	1	8	43
HOMO-2	−9.07	17	7	2	75

Table S4(a) Selective Kohn-Sham orbital contours of [**1**]$^{+}$ and **1**

[**1**]$^{+}$		
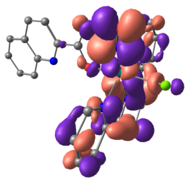	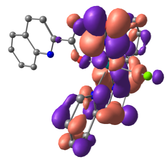	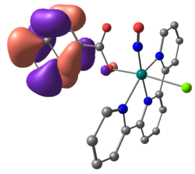
LUMO + 1	LUMO	HOMO
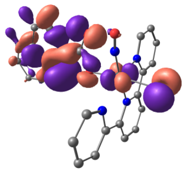	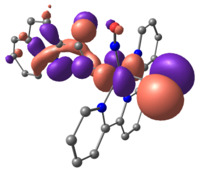	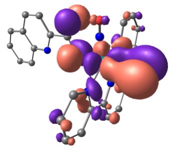
HOMO-2	HOMO-3	HOMO-6
1		
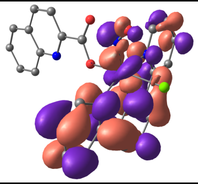	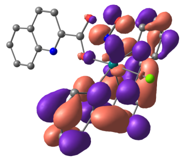	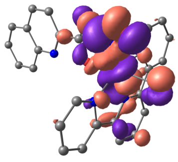
LUMO (α)	LUMO (β)	SOMO (α)

Table S4(b) Selective Kohn-Sham orbital contours of [**2**]$^{2+}$ and [**2**]$^{+}$

[**2**]$^{2+}$		
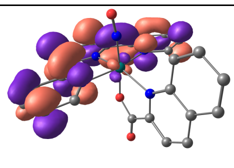	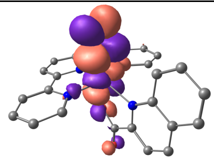	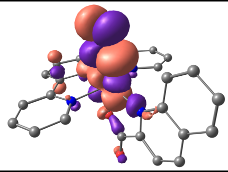
LUMO + 3	LUMO + 1	LUMO
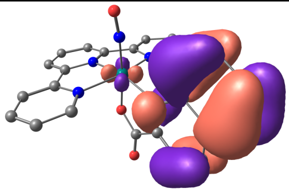	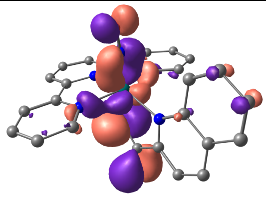	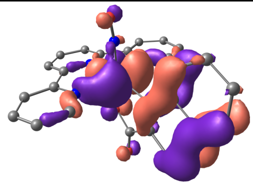
HOMO	HOMO-4	HOMO-5
[**2**]$^{+}$		
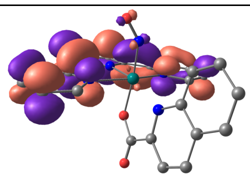	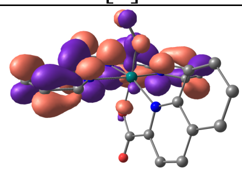	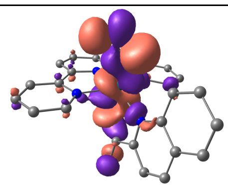
LUMO+1 (β)	LUMO (β)	SOMO (α)

Table S5 TD-DFT (B3LYP/CPCM) results for [**1**]$^+$, **1**

	E (eV)	λ(nm)	f	Transition	Character
[1]$^+$	2.73	454.20	0.0063	HOMO-3→LUMO (0.31) HOMO-2→LUMO (0.31)	Ru^{II}(dπ)/L(π)→NO$^+$(π*)
	3.42	363.01	0.0120	HOMO-6→LUMO (0.47)	Ru^{II}(dπ)/L(π)→NO$^+$(π*)
	3.68	337.27	0.0146	HOMO-5→LUMO+3 (0.50)	L(π)→NO$^+$(π*)/trpy(π*)
	3.77	328.67	0.0104	HOMO-8→LUMO+1 (0.47)	trpy(π)→NO$^+$(π*)
	4.08	304.00	0.0138	HOMO-9→LUMO+1 (0.55)	trpy(π)/Cl(π)→NO$^+$(π*)
1	2.20	562.44	0.0017	SOMO(α)→LUMO+1(α) (0.92)	Ru^{II}(dπ)/NO$^\bullet$(π)→trpy(π*)
	2.90	427.68	0.0014	SOMO(α)→LUMO+6(α) (0.61)	Ru^{II}(dπ)/NO$^\bullet$(π)→trpy(π*)
	3.34	371.06	0.0051	SOMO(α)→LUMO+6(α) (0.67)	Ru^{II}(dπ)/NO$^\bullet$(π)→trpy(π*)
	3.44	360.77	0.0046	HOMO-4(β)→LUMO(β) (0.75)	L(π)/Cl(π)→trpy(π*)
	3.73	332.16	0.0112	HOMO-6(β)→LUMO+5(β) (0.44)	L(π)→trpy(π*)/NO$^\bullet$(π*)
	3.87	320.27	0.0176	HOMO-4(β)→LUMO+1(β) (0.57)	L(π)/Cl(π)→trpy(π*)

Table S6 TD-DFT (B3LYP/CPCM) results for [**2**]$^{2+}$, [**2**]$^{+}$

	E (eV)	λ(nm)	*f*	Transition	Character
[**2**]$^{2+}$	3.58	346.21	0.0137	HOMO→LUMO+5 (0.39) HOMO→LUMO+3 (0.29)	Ru^{II}(dπ)/L(π)→NO^{+}(π*)
	3.72	333.33	0.0242	HOMO-5→LUMO (0.38)	Ru^{II}(dπ)/L(π)→NO^{+}(π*)
	4.23	292.70	0.0449	HOMO-4→LUMO+2 (0.40)	L(π)→trpy(π*)
	4.42	280.35	0.0482	HOMO-3→LUMO+2 (0.40)	L(π)→trpy(π*)
[**2**]$^{+}$	2.58	480.45	0.0032	SOMO(α)→LUMO+2(α) (0.96)	Ru^{II}(dπ)/NO$^{\bullet}$(π)→L(π*)
	3.33	372.29	0.0027	HOMO-4(α)→LUMO+1(α) (0.50)	Ru^{II}(dπ)/L(π)→trpy(π*)
	3.74	331.22	0.0186	HOMO-2(β)→LUMO+1(β) (0.40)	QA(π)→trpy(π*)
	3.77	329.22	0.0116	HOMO-2(β)→LUMO+4(β) (0.25)	QA(π)→trpy(π*)

Table S7 The selected bond order of $\{RuNO\}^n$, where n = 6,7

	N(5)-O(3)	Ru-N(5)	Ru-O(1)	Ru-N(3)	O(1)-C(1)	C(1)-O(2)
[**1**]$^+$	1.877	1.087	0.590	0.381	1.162	1.628
1	1.769	0.929	0.549	0.364	1.203	1.667
[**2**]$^{2+}$	1.834	1.084	0.687	0.484	1.009	1.919
[**2**]$^+$	1.750	0.915	0.585	0.472	1.110	1.877

(a)

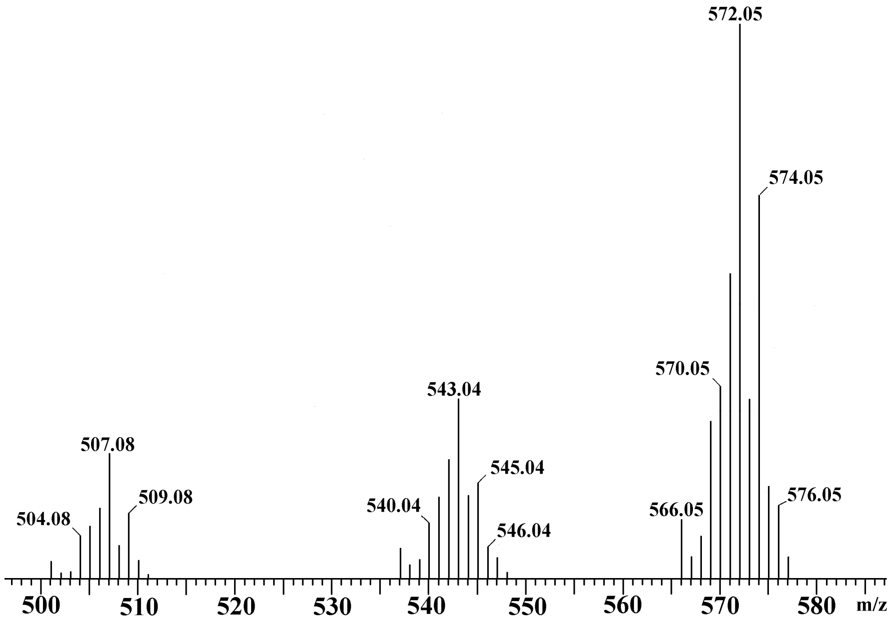

(b)

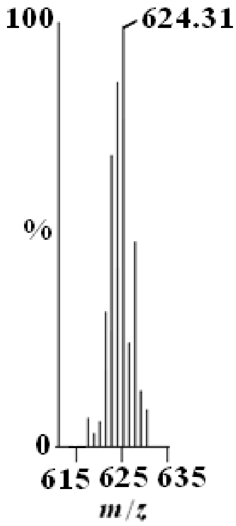

Fig. S1 ESI-MS(+) spectra of (a) [**1**]BF_4 and (b) [**2**]$(BF_4)_2$ in CH_3CN.

(a) (b)

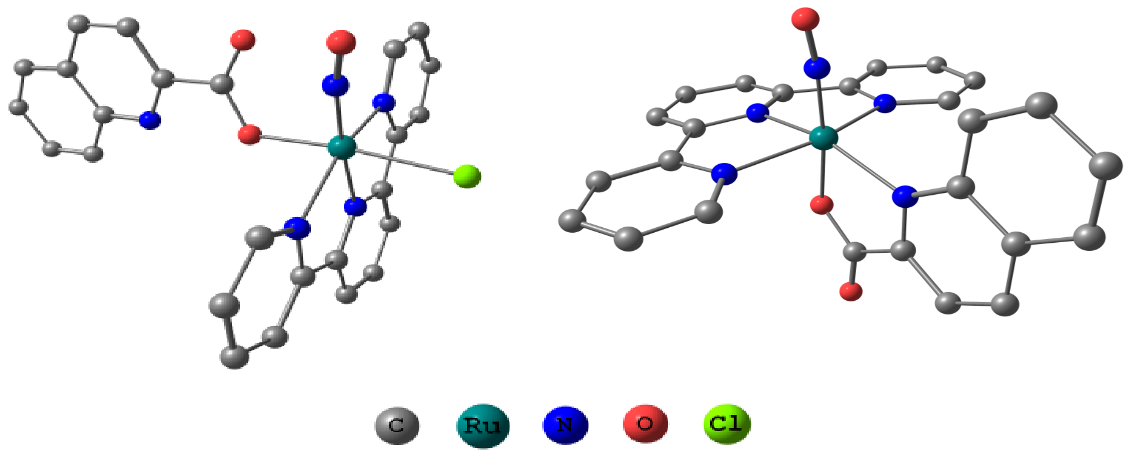

Fig S2 The DFT optimized geometries of (a) [**1**]$^{+}$ and (b) [**2**]$^{2+}$. The hydrogen atoms are omitted for clarity.

(a)

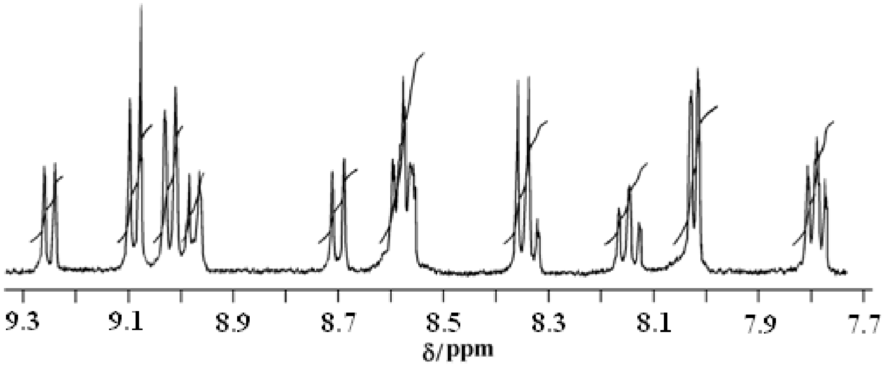

(b)

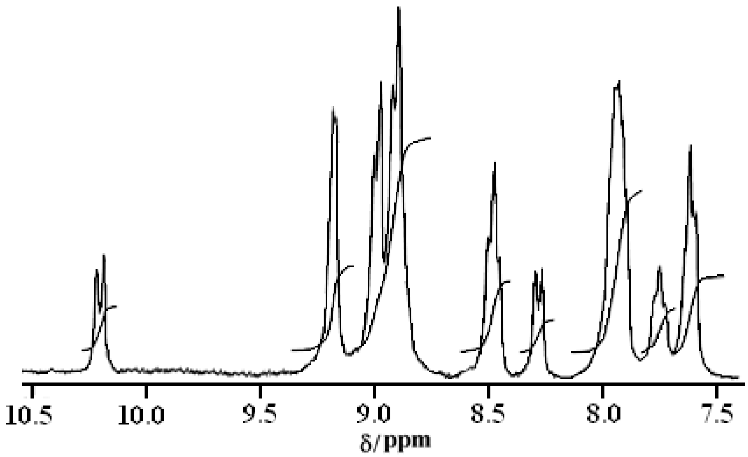

Fig. S3 ^{1}H NMR spectra of (a) [**1**]$^{+}$ and (b) [**2**]$^{2+}$ in $(CD_3)_2SO$.

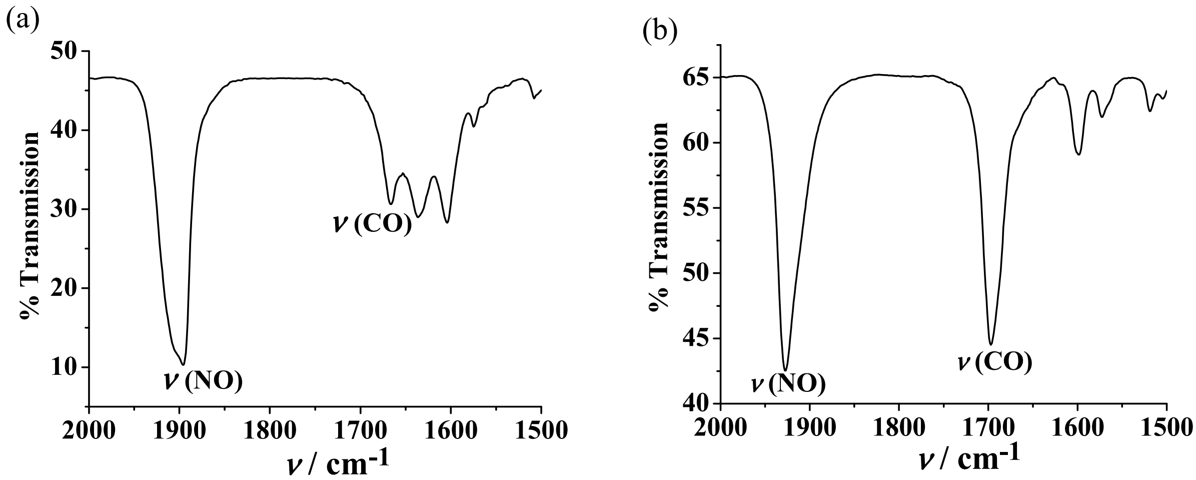

Fig. S4 IR spectra (KBr disk) of (a) [**1**]BF_4 and (b) [**2**]$(BF_4)_2$ in the region of 2000-1500 cm^{-1}.

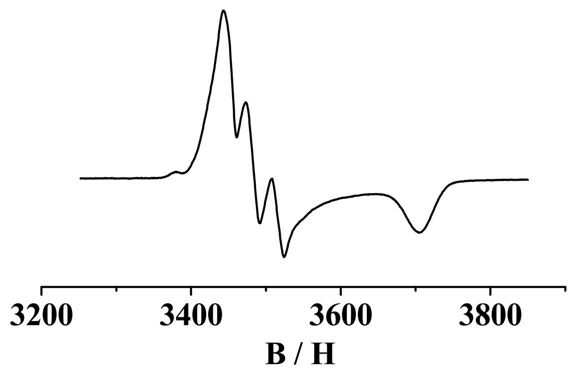

Fig. S5 EPR spectrum of [**2**]$^+$ in CH_3CN/0.1 M Bu_4NPF_6 solution at 110K.

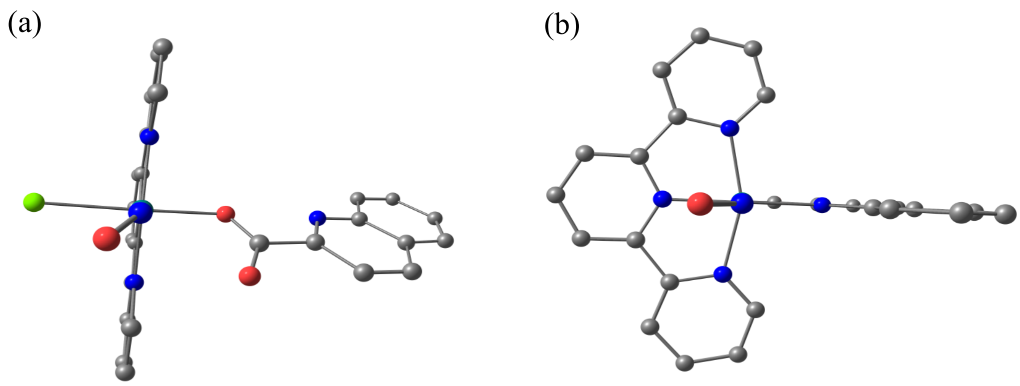

Fig. S6 The optimized geometry of (a) *pseudo*-staggered **1** and (b) eclipsed [**2**]$^+$.

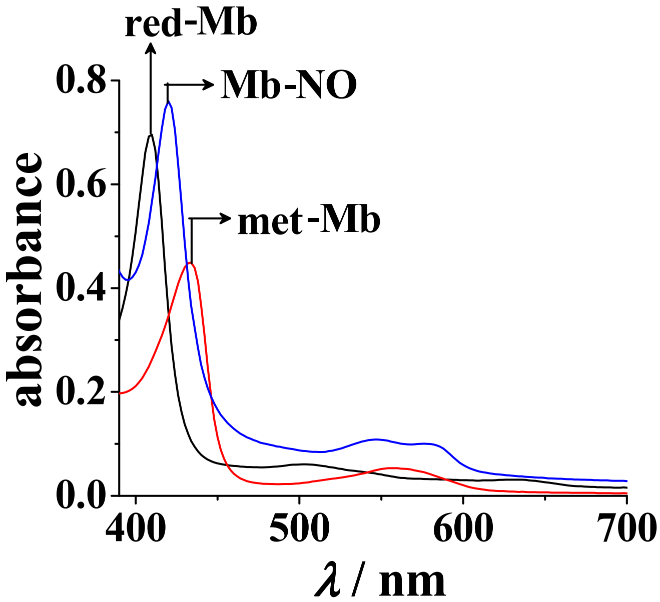

Fig. S7 Absorption spectra of met-*Mb*, reduced *Mb* and *Mb*-NO adduct in water.

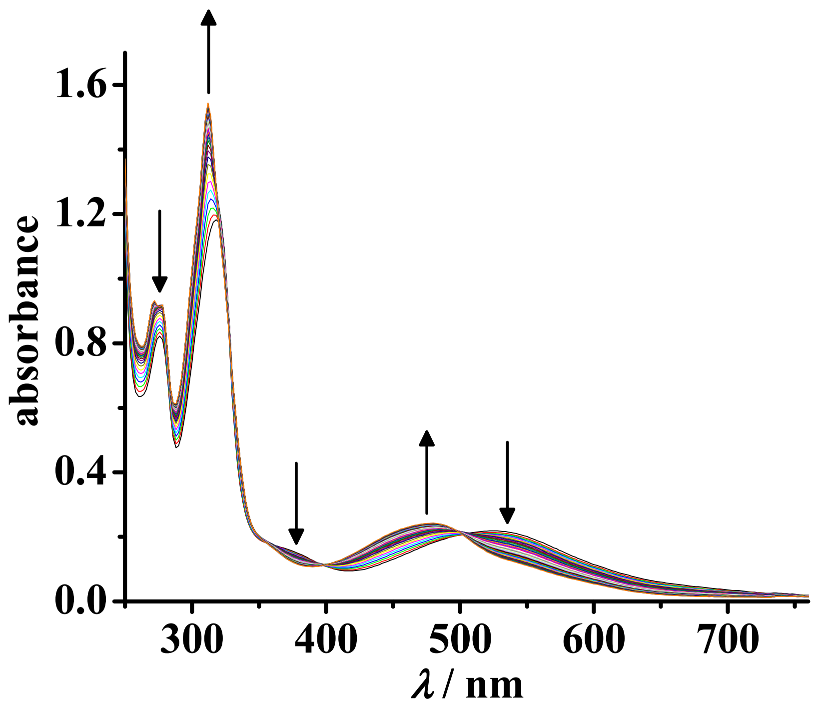

Fig. S8 The change in electronic spectral profile of [**1**] (0.68 x 10^{-4} M) in CH_3CN/0.1 M $HClO_4$ (pH ~ 1)) with time (5 min time intervals) under a steady flow of O_2.

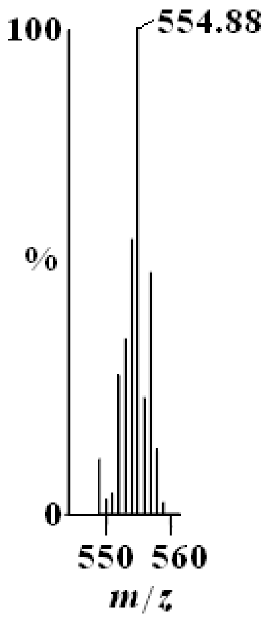

Fig. S9 ESI-MS(+) spectrum of $[(\mathbf{1a}\text{-Cl})+H]^+$ in CH_3CN.